

# Identifying the Key Issues in Inferior Performance of Quantum Rod LEDs

Zebing Liao\*, Maksym F. Prodanov\* , Mallem Kumar\*, Meiqi Sun\*, Ian Underwood\*\*\*, Abhishek Kumar Srivastava\*\*

\*1.State Key Laboratory of Advanced Displays and Optoelectronics Technologies, Department of Electronics and Computer Engineering, The Hong Kong University of Science and Technology, Hong Kong, 999077 China

\*\* .Centre for Display Research, Department of Electronics and Computer Engineering, The Hong Kong University of Science and Technology, Hong Kong, 999077 China

\*\*\* School of Engineering, Scottish Microelectronic Centre, The University of Edinburgh, Edinburgh EH9 3FB, UK

## Abstract

Quantum dot light-emitting diodes (QDLEDs) have approached the theoretical limit of external quantum efficiency (EQE) determined by outcoupling efficiency. To achieve further improvements, innovative optical designs must be explored. Quantum rod-based LEDs (QRLEDs) show great potential, offering a high transition dipole moment (TDM) orientation ratio of 80% to 90%, compared to 66.7% for isotropic QDs without complex alignment processes. However, significant performance gaps exist between QRLEDs and QDLEDs despite both types sharing similar core-shell structures and photoluminescence quantum yields (PLQY). In this paper, we identify a critical challenge: carrier leakage through irregular quantum rod films, which diminishes the EQE of QRLEDs and limits their competitiveness against QDLEDs. An equivalent circuit model consisting of two diodes effectively illustrates the impact of leakage current in conventional QDLED structures. By altering the QRLED device structure, we successfully improved balanced carrier injection while reducing the leakage current linked to the suboptimal QR layer. As a result, our QRLED achieved a maximum EQE of 30.2% (with an average of 28%) and a brightness of 110,000 cd/m<sup>2</sup>. These findings will pave the way for further advancements in the performance of LEDs based on anisotropic nanocrystals.

## Author Keywords

Quantum dot/rods, anisotropic nanocrystal, QLED, equivalent circuit model

## 1. Introduction

Since their discovery in the early 1980s, quantum dots (QDs) have emerged as highly promising materials for optoelectronic devices, including photodetectors, solar cells, light-emitting diodes (LEDs), and photocatalysts, thanks to their intrinsic properties derived from strong size-induced quantum confinement<sup>1,2</sup>. Among these applications, QDs have demonstrated significant potential for achieving high efficiency, brightness, and color purity in display technologies. However, the maximum external quantum efficiency (EQE) of red, green, and blue quantum dot LEDs (QDLEDs) has only surpassed theoretical limits of approximately 25 %, primarily due to near-unity internal quantum efficiency coupled with limited outcoupling efficiency<sup>3</sup>.

In typical device configurations, generated optical power is distributed across several modes, including waveguide, surface plasmon, substrate, and outcoupled modes. Unfortunately, nearly 80% of the emitted light becomes trapped within these multilayer thin-film devices. Researchers have proposed various strategies to mitigate this issue, such as refractive index matching, plasmonic enhancement, and the design of light scattering and outcoupling structures. However, these approaches often involve

complex nanofabrication processes that significantly increase costs or compromise overall device performance. Thus, more attractive alternatives should focus on overcoming outcoupling limitations to enhance performance without necessitating additional fabrication steps.

The elongated shape of quantum rods (QRs) imparts unique anisotropic properties that set them apart from QDs, including linearly polarized emission, faster radiative decay rates, and tunable Auger recombination rates<sup>4</sup>. The linearly polarized emission is particularly advantageous for QRs in photoluminescence and electroluminescence applications, as it facilitates horizontally aligned TDMs that can potentially double outcoupling efficiency without requiring additional fabrication processes. Our group recently demonstrated a 60% reduction in power consumption for liquid crystal displays using a photoaligned quantum rod as an enhancement film<sup>5</sup>. However, the performance of QRLEDs still lags behind that of QDLEDs, with limited reports on blue or green QLEDs exhibiting poor brightness and lifetime. To date, the highest EQE achieved for red QRLEDs is only 22%<sup>6</sup>, which remains significantly below the theoretical limit of 41% determined by outcoupling efficiency.

In this study, we investigated the key issues contributing to the poor performance of conventional structure LEDs based on quantum rods (QRs). The equivalent circuit model featuring two diodes demonstrates strong consistency and reveals that QRLEDs suffer significantly from large leakage currents, or non-radiative currents, compared to QDLEDs. The primary source of this difference stems from the less uniform quality of the QR layer, characterized by the presence of pinholes. By modifying the QRLED device structure, we were able to simultaneously enhance balanced carrier injections and suppress the leakage current associated with the suboptimal QR layer. The maximum EQE and brightness of our QRLED reached 30.2 % (with an average of 28%) and 110,000 cd/m<sup>2</sup>, respectively. We believe our research provides a pathway for improving the performance of LEDs that utilize irregularly shaped anisotropic nanocrystal emitters.

## 2. Discussion

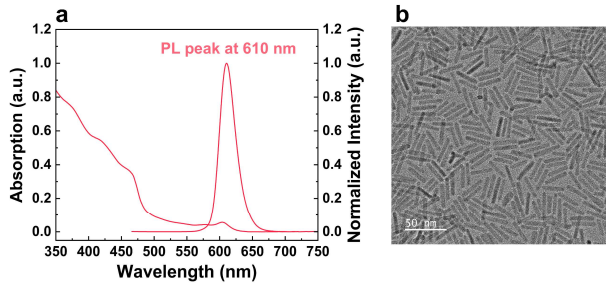


**Figure 1** a) The absorption and PL spectra of red QRs. b) The high-resolution TEM of QRs.

Red quantum rods were synthesized according to established protocols from previous studies. These rods, composed of a CdS core capped with a thin CdSe shell, exhibited an emission wavelength of 610 nm and a high photoluminescence yield of 92% in solution, with a narrow full width at half maximum (FWHM) of 30 nm, as shown in **Figure 1a**. High-resolution transmission electron microscopy (HRTEM) was utilized to analyze the micromorphology of the quantum rods, as illustrated in **Figure 1b**. The diameter and length of the red quantum rods were 28 nm and 4.5 nm, respectively, resulting in an aspect ratio of 6.2. The aspect ratio of quantum rods is critical for influencing the polarization of the emitted light; however, an increased aspect ratio may also lead to a decline in QRLED performance.

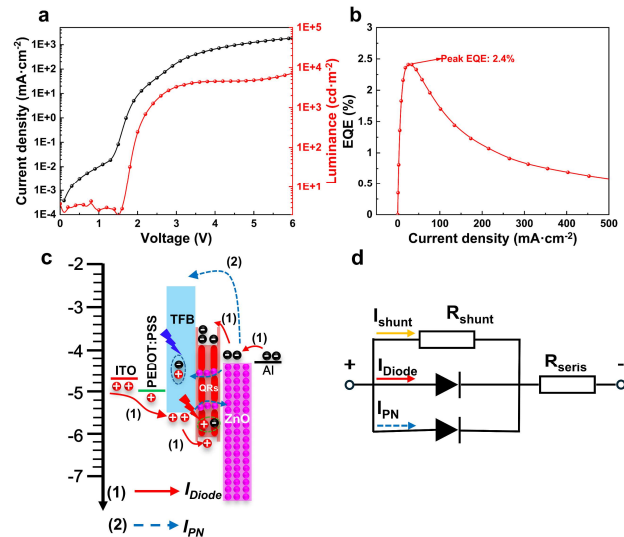


**Figure 2** a) The current-voltage-luminescence curve of red QRLED. b) The EQE versus the current density of red QRLED. c) Schematic representation of current flow within the TFB-based QRLED device, illustrating the PN junction current (indicated by blue dotted line arrows) and the diode current (indicated by red line arrows). The shunt current is not included in the energy diagram graph. d) The equivalent circuit model composing two diodes for the QRLED device operating mechanism.

We initially evaluated the optoelectronic performance of QRs in EL applications by constructing a QRLED device using a conventional device structure, which consisted of ITO/PEDOT:PSS(30 nm)/TFB (20 nm)/QRs (15 nm)/ZnO (55 nm)/Al (100 nm). However, the results were unsatisfactory, with the EQE reaching only 2.4%, as shown in **Figure 2a** and **2b**,

significantly below the theoretical value. To investigate the underlying mechanisms, we employed an equivalent circuit model featuring two diodes to analyze the current flow through the QRLED device, as illustrated in **Figure 2c** and **2d**. According to our proposed operating mechanism (**Figure 2c**), the total device current comprises three components: (1) the shunt current ( $I_{shunt}$ ), which is caused by intrinsic carriers within the functional layers driven by applied voltage; (2) the PN junction current ( $I_{PN}$ ), referring to the TFB and ZnO Schottky junction, which arises from bypass currents or short-circuit currents due to direct contact between TFB and ZnO, as indicated by the blue dotted arrow; and (3) the diode current ( $I_{diode}$ ), associated with radiative recombination and contributing to the overall EQE, as represented by the red solid arrow. The derivation based on classical Shockley theory becomes:

$$I = I_{shunt} + I_{diode} + I_{PN}$$

$$= \frac{V - R_{series} * I}{R_{shunt}} + I_0 \exp\left(\frac{q(V - R_{series} * I)}{akT}\right) + I_1 \exp\left(\frac{q(V - R_{series} * I)}{\beta kT}\right)$$

Where  $I_0$ ,  $I_1$  represents the dark saturation current of two diodes,  $kT/q$  is the thermal voltage, which is approximately 0.02586 V at room temperature;  $V$  represents the applied voltage upon the PN junction,  $R_{shunt}$  and  $R_{series}$  are the shunt resistors and series resistors, respectively.  $\alpha$  and  $\beta$  is the ideality factor of two diodes.

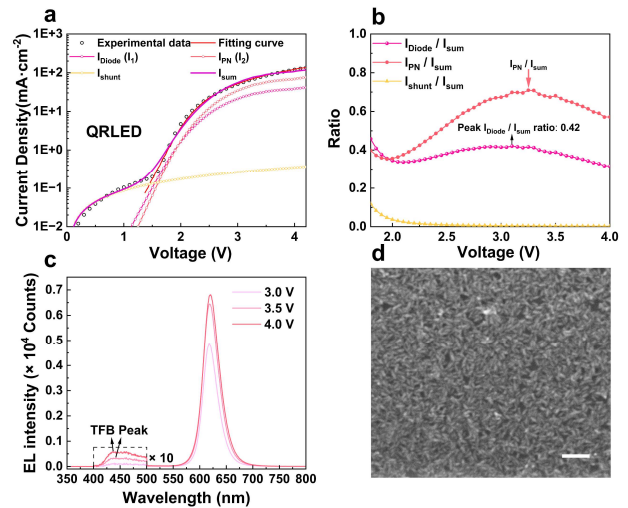


**Figure 3** a) JV curve fitting results for the QRLED, showing the calculated PN junction current and diode current based on the fitted parameters. b) The different current accounts for the total current flowing through the entire device. The black arrow indicates the peak ratio of  $I_{diode} / I_{sum}$ , the pink arrow indicates the peak ratio for  $I_{PN} / I_{sum}$  of QRLED, and the corresponding value at the same voltage for QDLED. c) The EL spectrum spectra at different applied biases for the QRLED and QDLED. d) The SEM image of the QRs layer on the ITO/PEDOT:PSS/TFB layer.

The fitting results, presented in **Figure 3a**, yielded an R-squared value of 0.998 for the TFB-based QRLED, indicating a strong correlation between the experimental data and our theoretical model, thereby validating our approach. The fitting results shown in **Figure 3b** reveal that the TFB-based conventional QRLED exhibits significantly larger shunt and PN junction currents, which account for over 60 % of the total current in the voltage range of 2.5 to 4 V. Furthermore, the ratio of the PN junction current to the total current shifts in accordance with changes in EL intensity from both parasitic emissions and QR emissions.

Specifically, the TFB emission (parasitic emission) peaks at 435 nm, while the QR emission (EL) peaks at 616 nm, as illustrated in **Figure 2c**. The scanning electron microscopy (SEM) images of the quantum rod (QR) films on the ITO/PEDOT: PSS/TFB layer further support the possibility of a large PN junction current ratio. The presence of pinholes in the film creates channels that facilitate direct contact between the TFB layer and ZnO.

To address the issues observed in our initial device, we constructed an inverted device with the following structure: ITO/ZnO (55 nm)/QRs (30 nm)/m-CBP (10 nm)/TCTA (50 nm)/Al (100 nm). The device schematic is illustrated in **Figure 4a**. Since the ZnO layer was fabricated prior to the application of the QRs, there was no interaction between the ZnO and QRs layers. Moreover, unlike the conventional device structure, the inverted configuration allows for the selection of a high-mobility hole transport layer (HTL) without concern for interactions with the underlying layers, effectively addressing the issue of insufficient hole injection. We utilized highly electron-conductive ZnO nanoparticles along with TCTA and m-CBP, which exhibit good hole mobility as the electron and hole transport layers, respectively. This combination aims to reduce the operating voltage and broaden the device's potential applications. **Figure 4b** displays the energy diagram of the QRLED. The valence and conduction band levels of the red were determined using ultraviolet photoelectron spectroscopy (UPS) and absorption spectroscopy. The conduction band of the red QRs was measured to be at 6.0 eV, consistent with previous reports. Given that the highest occupied molecular orbital (HOMO) of m-CBP is also situated at 6.0 eV, the energetic barrier for hole injection is negligible, facilitating carrier injection.

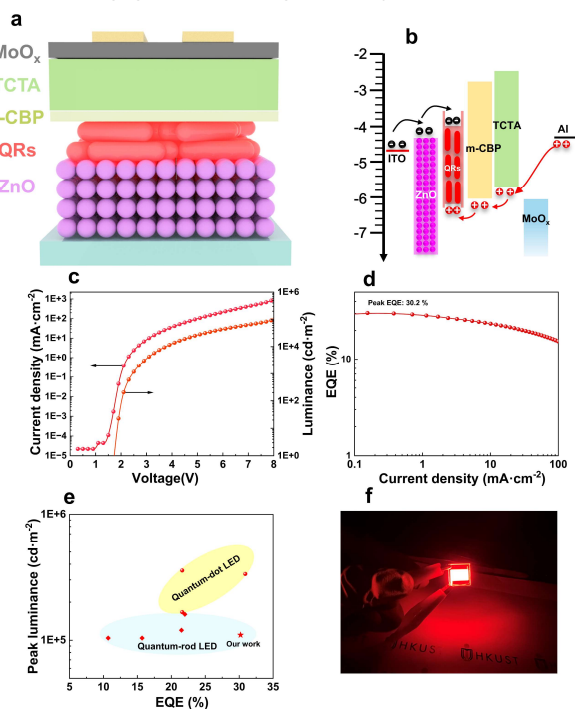


**Figure 4 a, b** Schematic diagram and energy diagram of the device structure. **c** The current density and luminance versus voltage. **d** The EQE versus current density. **e** comparison with the previously reported quantum dot LED, quantum well LED,

and quantum rod LED. **f** Photograph of operating large-area red QRLED, device area is 0.61 cm<sup>2</sup>.

The current-voltage-luminance characteristics of the inverted QRLED are presented in **Figure 4c**. The inverted QRLED exhibited significantly lower leakage current compared to the TFB-based forward QRLED device, measuring  $2 \times 10^{-3}$  mA/cm<sup>2</sup> at 1 V, in contrast to  $2 \times 10^{-1}$  mA/cm<sup>2</sup> for the TFB-based and m-CBP/TCTA devices. Furthermore, the inverted device demonstrated a much steeper slope in the current exponential increase region, indicating superior carrier injection capabilities. The peak EQE and brightness of our red QRLED reached 30.2% and 110,000 cd/m<sup>2</sup>, which is comparable to state-of-the-art solution-processed red QDLEDs and represents a record for red QRLEDs. Additionally, we fabricated a large-area device with a pixel area of 0.61 cm<sup>2</sup>, demonstrating high uniformity and brightness.

### 3. Conclusion

We investigated the factors contributing to the poor performance of conventional QRLED devices. The fitting results obtained using the equivalent circuit model clearly indicated that traditional TFB-based QRLEDs exhibit a significantly higher ratio of non-radiative recombination current under low bias conditions. This issue was addressed by developing an inverted device structure, which mitigates the penetration of high-mobility ZnO and enhances hole injection through precise tuning of the hole injection barriers. Furthermore, we achieved a record EQE of 30.2% (with an average of 28%) for red QRLEDs, along with impressive brightness levels reaching 110,000 cd/m<sup>2</sup>. We believe our findings offer a promising pathway to unlock the potential of anisotropic emitters in display and lighting applications.

### 4. Acknowledgments

Acknowledges the support from the RGC of Hong Kong SAR (Grant Nos. 26202019 and 16205623), an ITC grant, ITS/059/22MX, and the funding for The State Key Laboratory of Advanced Displays and Optoelectronics Technologies.

### 5. References

- Shen, H. et al. Visible quantum dot light-emitting diodes with simultaneous high brightness and efficiency. *Nature Photonics* 13, 192-197 (2019).
- García de Arquer, F. P. et al. Semiconductor quantum dots: Technological progress and future challenges. *Science* 373, eaaz8541 (2021).
- Liao, Z. et al. Ultralow roll-off quantum dot light-emitting diodes using engineered carrier injection layer. *Advanced Materials* 35, 2303950 (2023).
- Malle, K. et al. Solution-processed red, green, and blue quantum rod light-emitting diodes. *ACS Applied Materials & Interfaces* 14, 18723-18735 (2022).
- Kang, C. et al. Quantum-Rod On-Chip LEDs for Display Backlights with Efficacy of 149 lm W<sup>-1</sup>: A Step toward 200 lm W<sup>-1</sup>. *Advanced Materials* 33, 2104685 (2021).
- Zeng, Y. et al. 22% Record Efficiency in Nanorod Light-Emitting Diodes Achieved by Gradient Shells. *Advanced Materials* 36, 2310705 (2024).